Inorganic Chemistry

Article

pubs.acs.org/IC

Reversible Mechanochromic Luminescence at Room Temperature in Cationic Platinum(II) Terpyridyl Complexes

Ali Han,[†] Pingwu Du,*[,†] Zijun Sun,[†] Haotian Wu,[†] Hongxing Jia,[†] Rui Zhang,[‡] Zhenning Liang,[‡] Rui Cao,*[,‡] and Richard Eisenberg*[,§]

[†]Department of Chemistry, Department of Materials Science and Engineering, CAS Key Laboratory of Materials for Energy Conversion, University of Science and Technology of China, 96 Jinzhai Road, Hefei 230026, China

[‡]Department of Chemistry, Renmin University of China, 59 Zhongguancun Street, Beijing 100872, China

[§]Department of Chemistry, University of Rochester, New York 14623, United States

Supporting Information

ABSTRACT: Reversible mechanochromic luminescence in cationic platinum(II) terpyridyl complexes is described. The complexes $[Pt(Nttpy)Cl]X_2$ (Nttpy = 4′-(*p*-nicotinamide-*N*-methylphenyl)-2,2′:6′,2″-terpyridine, X = PF_6 (**1**), SbF_6 (**2**), Cl (**3**), ClO_4 (**4**), OTf (**5**), BF_4 (**6**)) exhibit different colors under ambient light in the solid state, going from red to orange to yellow. All of these complexes are brightly luminescent at both room temperature and 77 K. Upon gentle grinding, the yellow complexes (**4**–**6**) turn orange and exhibit bright red luminescence. The red luminescence can be changed back to yellow by the addition of a few drops of acetonitrile to the sample. Crystallographic studies of the yellow and red forms of complex **5** suggest that the mechanochromic response is likely the result of a change in intermolecular Pt···Pt distances upon grinding.

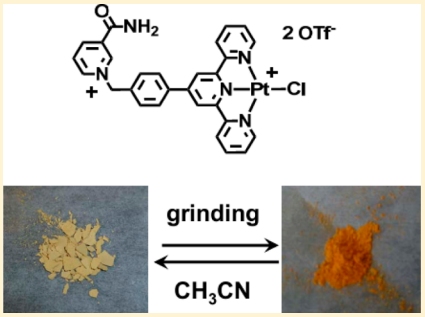

INTRODUCTION

Mechanochromism is an interesting phenomenon, characterized by changes of color *and/or* luminescence as a result of mechanical grinding or pressing of a sample in the solid state.[1,2] In the past decade, many materials based on organic dyes and compounds such as anthracene,[3,4] pyrene,[5,6] oligo(*p*-phenylene vinylene),[7−10] spiropyran,[11,12] and difluoroboron avobenzone[13] have been found to exhibit mechanochromic responses. The mechanochromism in these organic materials has been explained by the formation of different emissive aggregated states upon an external physical stimulus. In organometallic and metal complex chemistry, mechanochromic responses have also been explored as a consequence of metal···metal noncovalent interactions *and/or* intermolecular $\pi\cdots\pi$ interactions in several examples of silver,[14] gold,[15−18] and copper complexes.[19]

Square-planar cationic platinum(II) complexes have attracted great attention because of their rich photophysical and photochemical properties, including charge transfer absorptions in the visible region and solution emissive excited states. Applications of well-defined systems containing these platinum(II) complexes have been reported in a number of fields including photocatalysis,[20−23] light-emitting diodes (LEDs),[24] electroluminescence,[25] chemosensors,[26−30] biological labeling,[31,32] and solar cells.[33−35] During the past decade, cationic platinum(II) terpyridyl complexes have also been studied on the basis of their propensity to exhibit Pt···Pt *and/or* $\pi\cdots\pi$ interactions in the solid state.[36−47]

To obtain useful photoactive materials, the photoluminescent properties of candidate compounds must be controllable by external stimuli (pH, cations, anions, organic vapors, etc.), as has been found for cationic Pt(II) terpyridyl complexes. For example, vapochromism (a reversible change in absorption or emission color as a consequence of exposure to volatile organic compounds) has been described in a number of reports[43,44,48−50] of platinum(II) terpyridyl complexes in which the observed color change results from alterations in the Pt···Pt interactions in the solid state. However, to our best knowledge, no example of a cationic platinum(II) terpyridyl complex that exhibits mechanochromism has been reported in the literature. Although a few neutral platinum(II) bipyridyl complexes show mechanochromism,[51−53] no detailed crystallographic studies have been reported to identify the structural changes that occur upon grinding or other mechanical stimulation.

In the present study, we report the reversible mechanochromic luminescence of a cationic platinum(II) terpyridyl complex $[Pt(Nttpy)Cl]X_2$ (Scheme 1, where Nttpy = 4′-(*p*-nicotinamide-*N*-methylphenyl)-2,2′:6′,2″-terpyridine, and X = PF_6 (**1**), SbF_6 (**2**), Cl (**3**), ClO_4 (**4**), OTf (**5**), BF_4 (**6**)). All of these salts are brightly luminescent in the solid state at room temperature and 77 K, and their colors are found to depend on different counteranions. The orange salts **2** and **3** exhibit a vapochromic response to methanol, which is similar to that of **1**.[48] Interestingly, the yellow salts (**4**–**6**) show an interesting mechanochromic response upon gentle grinding.

Received: October 17, 2013
Published: March 11, 2014

   dx.doi.org/10.1021/ic402624u | *Inorg. Chem.* 2014, 53, 3338−3344

Scheme 1. Structures (top) and Colors (bottom) of Cationic Pt(II) Terpyridyl Complexes

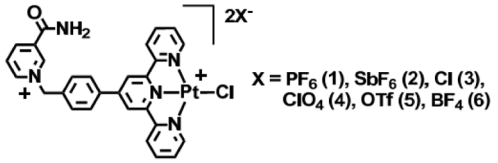

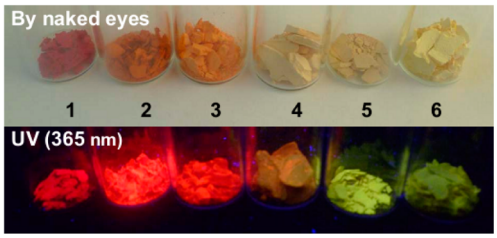

EXPERIMENTAL SECTION

Characterization. ^{1}H NMR spectra were recorded on a Bruker Avance 400 MHz spectrometer. Mass determinations were carried out by electrospray ionization mass spectrometry (ESI-MS) using a Thermal LCQ Fleet ion trap mass spectrometer. Absorption spectra were recorded using a Hitachi U2000 scanning spectrophotometer (200−1100 nm). The crystal phases and phase compositions of the powder samples were determined by a calibrated a Rigaku SmartLab X-ray powder diffractometer (CuKa graphite-monochromatized radiation, λ = 1.54178 Å, Regaku Denki Co. Ltd, Tokyo, Japan). The scanning rate was 5° min^{-1} in 2θ and peak positions were characterized by comparison with standard JCPDS files. Thermal-gravimetric analysis (TGA) experiments were performed using a Q5000IR Therml Analysis Instrument (TA Instrument, Inc., USA). Samples (1−3 mg) were placed in a alumina (Al_2O_3, 100 μL) pan and heated at a rate of 10 °C/min.

Luminescence. Luminescence spectra were obtained using a Spex Fluoromax-P fluorometer corrected for instrument response. Monochromators were positioned with a 2−5 nm band-pass. Solid-state emission samples were prepared as the solid state form of the complexes on a glass slide. The 77 K frozen samples were prepared in NMR tubes using a circular quartz-tipped immersion Dewar filled with liquid nitrogen for measuring the emission spectra. The pictures for color change were taken at room temperature when exposed to air.

Materials and Synthetic Methods. The chemicals dimethylformamide, methanol, sodium perchlorate, sodium triflate, sodium tetrafluoroborate, sodium hexafluoroantimonate, and Amberlite-TRA-400 ion-exchange resin were purchased (all from Aldrich) and used without further purification. The synthesis of 4′-(*p*-nicotinamide-*N*-methylphenyl)-2,2′:6′,2″-terpyridine (Nttpy) was conducted using a previously reported method.[48] All other reagents were of spectroscopic grade and used without further purification.

[Pt(Nttpy)Cl](PF$_6$)$_2$ (1). A 100 mL round-bottom flask was charged with 4′-(4-bromomethylphenyl)-2,2′:6′,2″-terpyridine (Br-ttpy, 0.35 g, 0.85 mmol), nicotinamide (0.14 g, 1.15 mmol), and 40 mL of dry acetonitrile. The resulting mixture was stirred at reflux for three days, and filtered through a medium porosity glass frit. The precipitate was washed with diethyl ether, and dried in vacuo. The above solid (75 mg, 0.142 mmol) and Pt(DMSO)Cl$_2$ (60 mg, 0.142 mmol) were then added into 15 mL of MeOH, and the mixture was refluxed at 70 °C for 6 h. A saturated $NaPF_6$ aqueous solution was then added into the suspension. The resulting mixture was stirred for 30 min at room temperature and filtered through a medium porosity glass frit, and the collected solids were washed with water and cold acetonitrile. Yield: 55% for two steps. The characterization data are consistent with the previous report.[48]

[Pt(Nttpy)Cl](SbF$_6$)$_2$ (2). Complex **2** was synthesized following the similar procedure as complex **1** except $NaSbF_6$ was used as the precipitating agent. The precipitate was collected by a frit and washed with water and cold acetonitrile to give the desired product. Yield: 62%. ^{1}H NMR (DMSO-d_6, ppm): 9.89 (s, 1H), 9.45 (d, 1H, J = 6.0 Hz), 9.10 (m, 3H), 8.85−8.94, (m, 4H), 8.80 (t, 1H, J = 6.2 Hz), 8.55 (t, 2H, J = 6.0 Hz), 8.30−8.35 (m, 3H), 8.20 (s, 1H), 7.90−7.96 (m, 4H), 6.05 (s, 2H). ESI-MS calcd for [M − SbF_6]$^+$ 910.79, [M − 2SbF_6]$^{2+}$ 337.52. Found [M − SbF_6]$^+$ 910.42, [M − 2SbF_6]$^{2+}$ 337.83. Anal. Found (%): C, 28.95; H, 2.32; N, 6.42. Calcd (%) for $C_{28}H_{22}ClF_{12}N_5OPtSb_2\cdot H_2O\cdot 0.25CH_3CN$: C, 29.14; H, 2.12; N, 6.26.

[Pt(Nttpy)Cl]Cl$_2$ (3). Complex **1** (100 mg, 0.10 mmol) was added into a mixed solvent containing methanol and water (50 mL, v/v = 1:1), and the suspension was treated with Amberlite-TRA-400 ion-exchange resin in the chloride form to give a clear red solution of the dichloride salt of the complex. After filtration of the solution to remove the resin, the filtrate was evaporated, and the residue was washed with water and cold acetonitrile, to give the desired product (64 mg, 83%). ^{1}H NMR (DMSO-d_6, ppm): 9.89 (s, 1H), 9.45 (d, 1H, J = 6.0 Hz), 9.10 (m, 3H), 8.85−8.94, (m, 4H), 8.80 (s, 1H), 8.55 (t, 2H, J = 6.0 Hz), 8.30−8.35 (m, 3H), 8.20 (s, 1H), 7.90−7.96 (m, 4H), 6.05 (s, 2H). ESI-MS calcd for [M − Cl]$^+$ 710.50, [M − 2Cl]$^{2+}$ 337.52. Found [M − Cl]$^+$ 709.83, [M − 2Cl]$^{2+}$ 337.67. Anal. Found (%): C, 45.10; H, 3.44; N, 9.28. Calcd for $C_{28}H_{22}Cl_3N_5OPt\cdot 0.5CH_3OH$: C, 44.92; H, 3.17; N, 9.19.

[Pt(Nttpy)Cl](ClO$_4$)$_2$ (4). The procedure is similar to the synthesis of complex **2**. The salt used for metathesis is $NaClO_4$. (***Caution!*** *Perchlorate salts are potentially explosive and should be handled with care and in small amounts.*) Yield: 69%. ^{1}H NMR (DMSO-d_6, ppm): 9.70 (s, 1H), 9.36 (d, 1H, J = 4.0 Hz), 8.95−9.05 (m, 5H), 8.83, (d, 2H, J = 8.4 Hz), 8.55−8.60 (m, 3H), 8.35 (t, 1H, J = 5.0 Hz), 8.27 (d, 2H, J = 7.5 Hz), 8.20 (s, 1H), 7.97 (t, 2H, J = 4.0 Hz), 7.89 (d, 2H, J = 5.0 Hz), 6.05 (s, 2H). ESI-MS calcd for [M − ClO_4]$^+$ 774.49, [M − 2ClO_4]$^{2+}$ 337.52. Found [M − ClO_4]$^+$ 774.08, [M − 2ClO_4]$^{2+}$ 337.67. Anal. Found (%): C, 39.12; H, 2.48; N, 8.40. Calcd for $C_{28}H_{22}Cl_3N_5O_9Pt\cdot 0.5CH_3CN$: C, 38.94; H, 2.65; N, 8.61.

[Pt(Nttpy)Cl](OTf)$_2$ (5). The procedure is similar to the synthesis of complex **2**. The salt used for metathesis is NaOTf. Yield: 67%. ^{1}H NMR (DMSO-d_6, ppm): 9.69 (s, 1H), 9.36 (d, 1H, J = 5.0 Hz), 8.95−9.05 (m, 5H), 8.84, (m, 2H), 8.55−8.62 (m, 3H), 8.35 (t, 1H, J = 6.0 Hz), 8.27 (d, 2H, J = 7.0 Hz), 8.20 (s, 1H), 7.99 (m, 2H), 7.88 (d, 2H, J = 7.4 Hz), 6.05 (s, 2H). ESI-MS calcd for [M − OTf]$^+$ 824.11, [M − 2OTf]$^{2+}$ 337.52. Found [M − OTf]$^+$ 823.92, [M − 2OTf]$^{2+}$ 337.58. Anal. Found (%): C, 37.28; H, 2.15; N, 7.52. Calcd for $C_{30}H_{22}ClF_6N_5O_7PtS_2$: C, 37.03; H, 2.28; N, 7.20.

[Pt(Nttpy)Cl](BF$_4$)$_2$ (6). The procedure is similar to the synthesis of complex **2**. The salt used for metathesis is $NaBF_4$. Yield: 55%. ^{1}H NMR (DMSO-d_6, ppm): 9.69 (s, 1H), 9.38 (d, 1H, J = 5.2 Hz), 8.95−9.05, (m, 5H), 8.85 (d, 2H, J = 6.0 Hz), 8.63 (s, 1H), 8.59 (t, 2H, J = 7.0 Hz), 8.37 (t, 1H, J = 5.0 Hz), 8.29 (d, 2H, J = 6.4 Hz), 8.22 (s, 1H), 8.00 (t, 2H, J = 6.0 Hz), 7.90 (d, 2H, J = 5.0 Hz), 6.05 (s, 2H). ESI-MS calcd for [M − BF_4]$^+$ 761.85, [M − 2BF_4]$^{2+}$ 337.52. Found [M − BF_4]$^+$ 761.00, [M − 2BF_4]$^{2+}$ 337.58. Anal. Found (%): C, 39.44; H, 2.40; N, 8.55. Calcd for $C_{28}H_{22}B_2ClF_8N_5OPt$: C, 39.63; H, 2.61; N, 8.25.

X-ray Structural Determinations of the Yellow and Red Forms of [Pt(Nttpy)Cl](OTf)$_2$ (5). Yellow crystals of [Pt(Nttpy)Cl](OTf)$_2$ (**5-Y**) suitable for single crystal X-ray diffraction were grown by the slow diffusion of diethyl ether into a concentrated solution of [Pt(Nttpy)Cl](OTf)$_2$ (**5**) in acetonitrile at ambient temperature. A yellow crystal (0.06 × 0.05 × 0.05 mm^3) was placed onto the tip of a glass fiber and mounted on a Bruker SMART APEX II CCD Platform diffractometer for data collection at 100.0(1) K.[54] Data collection was carried out using Mo Kα radiation (graphite monochromator) with a frame time of 90 s and a detector distance of 5.00 cm. Red crystals of [Pt(Nttpy)Cl](OTf)$_2$ (**5-R**) suitable for single crystal X-ray diffraction were grown by the slow diffusion of diethyl ether into a concentrated solution of [Pt(Nttpy)Cl](OTf)$_2$ (**5**) in methanol at ambient temperature. The red crystal (0.26 × 0.08 × 0.04 mm^3) was placed onto the tip of a glass fiber and mounted on a Bruker SMART APEX II CCD Platform diffractometer for a data collection at 100.0(1) K.[54] The initial sets of frames were oriented such that orthogonal wedges of reciprocal space were surveyed. The space groups were assigned as $P\bar{1}$ for both **5-Y** and **5-R**. Both structures were solved by direct methods

dx.doi.org/10.1021/ic402624u | Inorg. Chem. 2014, 53, 3338−3344

and refined employing full-matrix least-squares on F^2 (Bruker-AXS, SHELXTL-97).[55] All non-hydrogen atoms were refined with anisotropic displacement parameters. All hydrogen atoms were placed in ideal positions and refined as riding atoms with relative isotropic displacement parameters. For **5-Y**, the final full matrix least-squares refinement converged to R1 = 0.0284 (F^2, $I > 2\sigma(I)$) and wR2 = 0.0603 (F^2, all data). For **5-R**, the final full matrix least-squares refinement converged to R1 = 0.0199 (F^2, $I > 2\sigma(I)$) and wR2 = 0.0521 (F^2, all data).

RESULTS AND DISCUSSION

For the preparation and isolation of **1**−**2** and **4**−**6**, anion exchange experiments followed the protocol of stirring the water-soluble complex with different sodium salts in water/methanol mixtures.[44,48] The precipitate was collected and washed with cold acetonitrile, leading to the formation of the target complexes (see Experimental Section). Complex **3** was synthesized by anion exchange with Amberlite-TRA-400 ion-exchange resin in the chloride form. All the complexes were characterized by ^{1}H NMR spectroscopy, mass spectrometry, and elemental analyses.

The different salts **1**−**6** show nearly identical UV−vis absorption spectra in dilute solutions (Figure 1) with the

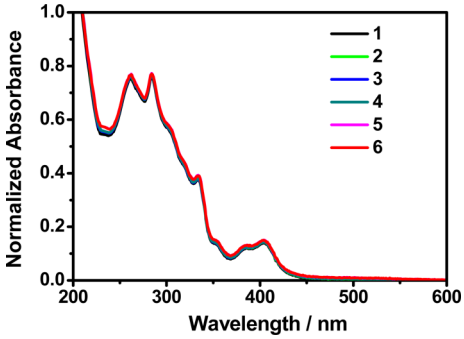

Figure 1. Normalized absorption spectra of complex **1**−**6** in acetonitrile under 1.0×10^{-5} M at room temperature.

$[Pt(Nttpy)Cl]^{2+}$ cation showing a broad low-energy absorption between 365 and 450 nm with λ_{abs}^{max} at 384 and 404 nm ($\varepsilon \sim 3700$ dm^3 mol^{-1} cm^{-1}), possibly corresponding to the $d\pi(Pt)-\pi(terpy)$ metal-to-ligand charge transfer (MLCT) transition resulting from the promotion of an electron from a Pt(d) HOMO to the LUMO which is a π^* orbital on the terpyridyl ligand.[56,57] The anions have no appreciable effect on the absorption properties of the different salts in dilute solutions. The absorption bands in the range 200−365 nm correspond to spin-allowed intraligand ($\pi-\pi^*$) transitions ($\varepsilon > 2 \times 10^4$ dm^3 mol^{-1} cm^{-1}). A linear plot of absorbance at 404 nm versus the concentration of complex **5** (OTf^- as the counteranion) in acetonitrile (less than 5.5×10^{-5} M) demonstrates that this absorption band does obey the Beer−Lambert law, indicating the absence of Pt···Pt *and/or* $\pi\cdots\pi$ interactions in dilute solutions (Figure S1, Supporting Information).[36,58] All of the salts are not emissive in dilute solutions at room temperature, which is also consistent with a previous report.[48]

Solid samples of compounds **1**−**6** with different counteranions, however, exhibit different colors, as illustrated in Scheme 1. The luminescence spectra of **1**−**6** in the solid state at room temperature are shown in Figure 2, top, with maximum wavelengths (λ_{em}^{max}) at 634, 613, 603, 517, 521, and 517 nm,

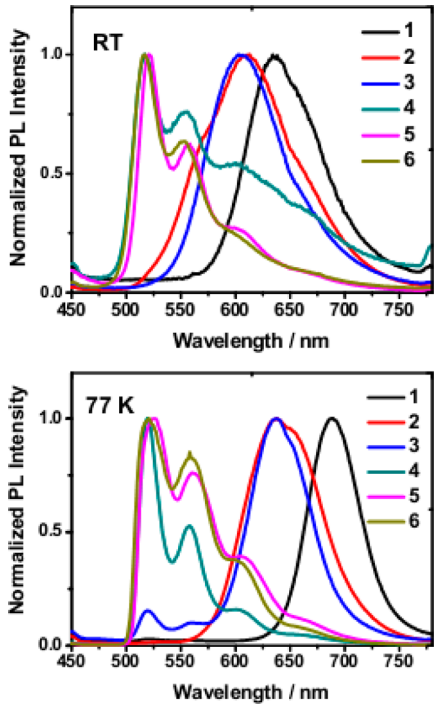

Figure 2. Emission spectra of complex **1**−**6** in the solid state at room temperature (top) and at 77 K (bottom). The excitation wavelength is 420 nm.

respectively. Compound **5** exhibits two emission shoulders at 557 and 599 nm. Compound **6** has a very similar emission structure, but it is shifted slightly to higher energy by 3 nm (~97 cm^{-1}). For compound **4**, there is only one obvious shoulder peak maximized at 554 nm and a broad emissive band between 580 and 750 nm, resulting in an orange color. In contrast, for salts **1**−**3**, the emission band at room temperature is relatively broad and featureless with no obvious shoulders. At 77 K, all of these salts show red-shifted emission spectra, with maximum wavelengths at 687, 638, 638, 519, 525, and 519 nm, respectively. Although **4**−**6** have only slight shifts to lower energy by 2−4 nm (~74−147 cm^{-1}) relative to their room-temperature spectra, significant red shifts are seen for **1**−**3** upon cooling to 77 K, with differences ranging from 25 to 53 nm (~910−1217 cm^{-1}), indicating that temperature has a big effect on the broad, featureless emission assigned as the metal−metal-to-ligand charge transfer (MMLCT) described below.[36]

Interestingly, after a gentle grinding of **4**−**6** using a pestle, all of these yellow luminescent salts exhibit bright red luminescence under UV irradiation at 365 nm from a hand-held UV lamp. Upon treatment of the ground powder with a few drops of acetonitrile, the red luminescence from these complexes changes back to the original yellow luminescence after drying of the solid in air for a few minutes. The yellow luminescence of **4**−**6** can again be changed to red luminescence upon grinding, and this process can be repeated many times without substantial chemical degradation of the starting materials. The results thus indicate good reversibility of mechanochromism in the salts of this cationic Pt(II) terpyridyl complex. The mechanochromic response was recorded by steady-state spectroscopy as shown in Figure 3 for the triflate salt **5** as an example. Before grinding, complex **5** has very similar emission bands at room temperature and 77 K maximized at 520 and 525 nm, respectively. After thorough

dx.doi.org/10.1021/ic402624u | Inorg. Chem. 2014, 53, 3338−3344

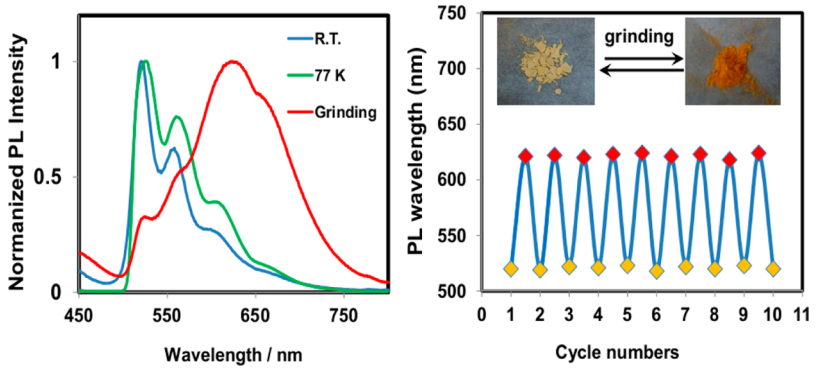

Figure 3. Emission spectra of complex **5** before and after gentle grinding (left). Color change of complex **5** during grinding and the reversibility of mechanochromic response (right), the maximum emission intensity of **5-Y** (λ_{em}^{max} = 520 nm) and **5-R** (λ_{em}^{max} = 621 nm) vs cycle numbers. The excitation wavelength is 420 nm.

grinding of the yellow powder, a red-orange powder is formed, and it exhibits a bright red luminescence with a maximum peak at 621 nm. The reversibility of this mechanochromic process for 10 cycles is shown on the right in Figure 3. Both **4** and **6** demonstrate similar mechanochromic responses as complex **5** does, and their photophysical properties in the solid state are shown in Supporting Information Figures S2 and S3.

The luminescent decay profiles of complex **5-Y** (yellow form) and **5-R** (red form) in the solid state have been examined at room temperature (Figure 4). The data of **5-Y** fit a two

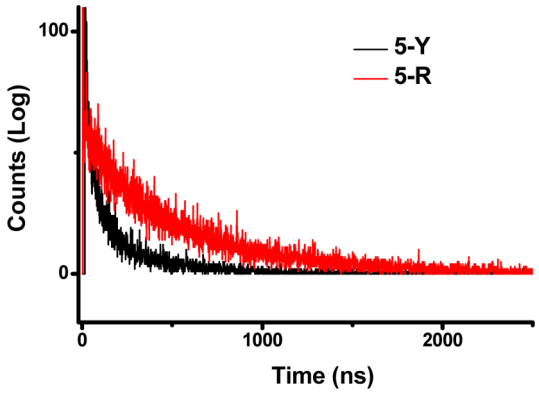

Figure 4. Luminescent decay of complex **5** in solid state before (black) and after (red) gentle grinding at room temperature. The excitation wavelength is 400 nm.

exponential decay function, and its excited-state lifetimes are 0.16 and 0.80 μs. However, the excited-state decay of **5-R** fits one exponential function, and its lifetime is 0.42 μs. The significant difference in excited-state lifetimes indicates that a transformation from one form to the other has occurred upon mechanical grinding.

Single crystal X-ray crystal structures of complex **5** have been determined for both red form and yellow form. Crystallographic data and detailed information can be found in the Supporting Information. Crystals of **5-Y** (yellow form) were obtained by slow diffusion of diethyl ether into a concentrated solution of the complex in acetonitrile, and crystals of **5-R** (red form) were afforded by slow diffusion of ether into a concentrated methanol solution. The molecular structure of the cationic moiety of **5-Y** is shown in Figure S4 in the Supporting Information. The N(1)−Pt−N(2) "trans" angle is 162.24(14)°, and the Pt−N distances range from 1.930(3) to 2.020(4) Å with the central nitrogen having the shortest distance. The distortion from a square planar coordination geometry is imposed by the "small-bite" constraints of the terpyridyl ligand. The Pt−Cl bond distance is 2.2942(11) Å. Other bond distances and angles are similar to corresponding metrical parameters reported for **1** and other cationic platinum(II) terpyridyl complexes.[26−29,37,38,48,59−62] The molecular structure of the cationic moiety of **5-R** is shown in Supporting Information Figure S5, which shows very similar bond lengths and angles to **5-Y**. Table S1−S6 in the Supporting Information list important bond lengths and angles for both the yellow (**5-Y**) and red (**5-R**) crystalline forms.

Figure 5 shows the packing arrangements for both **5-Y** and **5-R**, revealing that for both forms the cationic Pt(II) complexes are stacked in a head-to-tail orientation with two alternating distances between adjacent complexes. There are small-to-

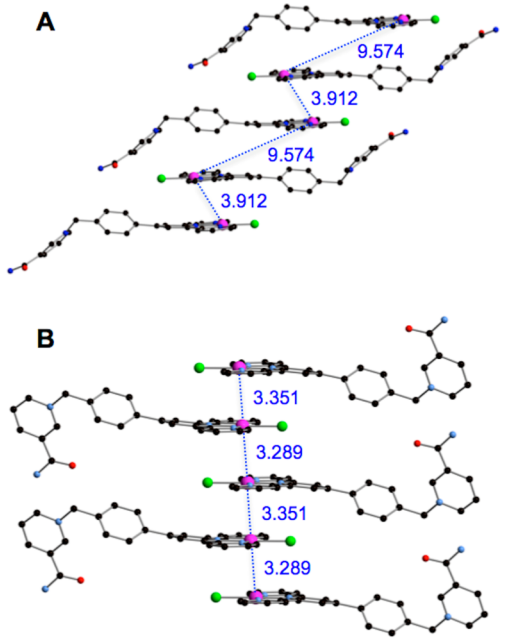

Figure 5. Stacking diagrams depicting the Pt···Pt distances and nonlinear (83.49°) angle between Pt atoms in **5-Y** (A) and the pseudolinear (176.00°) arrangement in **5-R** (B). Hydrogen atoms and solvent molecules are omitted for clarity. The colors of different atoms are black (carbon), pink (platinum), green (chloride), red (oxygen), and blue (nitrogen).

dx.doi.org/10.1021/ic402624u | Inorg. Chem. 2014, 53, 3338−3344

negligible $\pi-\pi$ interactions in both forms, as evidenced by the perpendicular distances of 3.50 and 3.62 Å between neighboring terpyridyl ligands in **5-Y**, and the minimal direct overlap of terpyridyl C atoms when viewed down the stacking direction (see Figures S6 and S7 in the Supporting Information). In **5-Y** form, the Pt···Pt distances are 3.912 and 9.574 Å, and Pt···Pt···Pt angle is 83.49°, indicating no significant metallophilic interactions in the solid structure. The effective overlap of nearest neighbor Pt d_{z^2} and p_z orbitals, that are the basis of metallophilic interactions, can be excluded by the long Pt···Pt distances within the cation stacking arrangement.[63]

The cationic packing of **5-R** is different from that of **5-Y**, as illustrated in Figure 5B. The calculated crystal density of **5-Y** is 2.014 mg/m^3. However, the value is decreased to 1.911 mg/m^3 for **5-R**, indicating grinding of the yellow form of **5** caused the slipping of layers and resulted in a less dense form. The stacking of the planar complexes in **5-R** has the same orientation as **5-Y** but shows much shorter Pt···Pt distances. These short Pt···Pt separations are 3.351 and 3.289 Å, and the arrangement of the complexes containing these Pt(II) ions suggests that metallophilic bonding (<3.5 Å[40]) in the crystal occurs through d_{z^2} and p_z overlap interactions with configuration interaction (d_{z^2} and p_z mixing) that leads to a change in the nature of the HOMO of these systems to reflect the metallophilic interaction. The resultant decrease in the shorter Pt···Pt interaction and the consequent red shift of the emission of **5-R** relative to **5-Y** is thus a consequence of the change in the nature of the HOMO to a mixed metal orbital (MM) and the designation of the emissive state to ^{3}MMLCT.[36] It is noteworthy to mention that no solvent molecules were found in the crystal lattice of the red form complex **5-R**. In addition, we examined the crystal structure, but there are no void spaces compatible with acetonitrile. Therefore, the reverse color change from red to yellow might not result from the change of crystal lattice induced by the insertion of solvent molecules. However, complex **5** is soluble in acetonitrile. After gentle grinding, the addition of a certain amount of acetonitrile into the powder may initiate the recrystallization process to change its color back to yellow.

Powder X-ray diffraction (XRD) data were further collected (Figure 6). The XRD pattern of the unground sample (**5-Y**) shows good reflection peaks that are in agreement with the simulated pattern from its single crystals (Figure 6, top). In contrast, there are significant decreased peak intensities with increased peak widths in the XRD pattern of the ground sample (**5-R**, Figure 6, bottom). The XRD differences of unground and ground samples likely result from a crystal-to-amorphous phase conversion upon grinding. More powder XRD data were collected to check the reversibility of phase conversion upon grinding, as shown in Figure S8. When a few drops of acetonitrile was added to the ground sample (**5-R**), the reflection peaks in plot C that are in agreement with the unground sample (**5-Y**) were clearly recovered, which is nearly identical to plot A in Figure S8. When the dry sample in plot C was further treated by gentle grinding, the powder phases in plot C showed amorphous character with significant decreased peak intensities, as shown in plot D. These results indicate that the powder materials of compound **5** exhibit good reversibility during mechanochromism. The thermal stability of the yellow and red forms of complex **5** and complex **3** were probed by thermal gravimetric analysis (Figure S9 in the Supporting Information). The results display only a very minor (<1.80%) mass loss for these three complexes up to approximately 165 °C, indicating that the complexes have good stability at normal temperature.

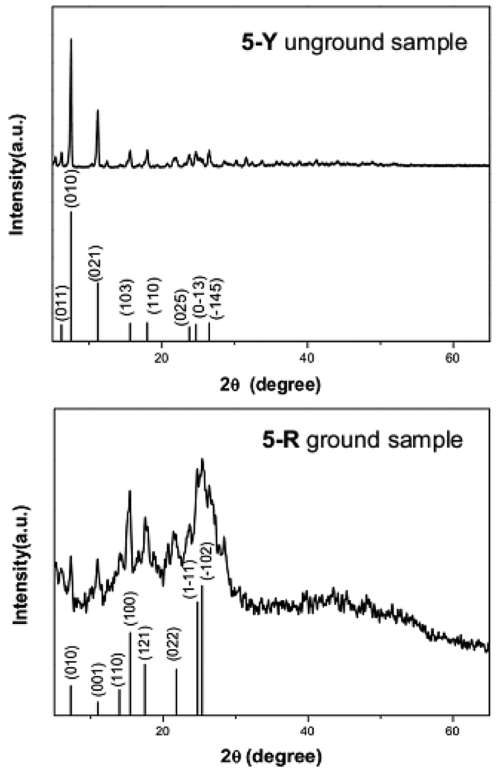

Figure 6. Powder X-ray diffraction (XRD) patterns of complex **5** in the solid state before (top) and after (bottom) gentle grinding at room temperature. The patterns in each figure at the bottom are calculated data.

CONCLUSIONS

In conclusion, we have described the reversible mechanochromic luminescence effect for different salts of a cationic Pt(II) terpyridyl complex in the solid state. In [Pt(Nttpy)Cl]X_2, the solid samples exhibit yellow color and yellow luminescence under ambient light when the anions are ClO_4^-, OTf^-, and BF_4^-. Upon gentle grinding of these salts at room temperature, the yellow luminescence changes to a bright red luminescence, a process that can be reversed repeatedly. The emission color change is clearly evidenced by single crystal X-ray diffraction studies of complex **5** in two different forms. The red crystals of **5** (**5-R**) show short Pt···Pt distances (<3.5 Å), indicating metallophilic interactions, contributing to red luminescence whereas the yellow form of **5** (**5-Y**) lacks significant metallophilic interactions due to long Pt···Pt distances (>3.9 Å).

ASSOCIATED CONTENT

Supporting Information

Additional characterization data and figures. Crystallographic data in CIF format. This material is available free of charge via the Internet at http://pubs.acs.org.

AUTHOR INFORMATION

Corresponding Authors

*E-mail: dupingwu@ustc.edu.cn.
*E-mail: ruicao@ruc.edu.cn.

*E-mail: eisenberg@chem.rochester.edu.

Notes

The authors declare no competing financial interest.

■ ACKNOWLEDGMENTS

This work was financially supported by the National Natural Science Foundation of China (No. 21271166 to P.D. and 21101170 to R.C.) and 1000 Young Talented Program. P.D. also acknowledges support from the Fundamental Research Funds for the Central Universities, and Program for New Century Excellent Talents in University (NCET). R.E. wishes to acknowledge the Division of Chemical Sciences, Geosciences, and Biosciences, Office of Basic Energy Sciences, U.S. Department of Energy, Grant DE-FG02-09ER16121 for funding.

■ REFERENCES

(1) Sagara, Y.; Kato, T. *Nat. Chem.* **2009**, *1*, 605.
(2) Balch, A. L. *Angew. Chem., Int. Ed.* **2009**, *48*, 2641.
(3) Sagara, Y.; Kato, T. *Angew. Chem., Int. Ed.* **2011**, *50*, 9128.
(4) Sagara, Y.; Yamane, S.; Mutai, T.; Araki, K.; Kato, T. *Adv. Funct. Mater.* **2009**, *19*, 1869.
(5) Sagara, Y.; Kato, T. *Angew. Chem., Int. Ed.* **2008**, *47*, 5175.
(6) Sagara, Y.; Mutai, T.; Yoshikawa, I.; Araki, K. *J. Am. Chem. Soc.* **2007**, *129*, 1520.
(7) Löwe, C.; Weder, C. *Adv. Mater.* **2002**, *14*, 1625.
(8) Crenshaw, B. R.; Weder, C. *Chem. Mater.* **2003**, *15*, 4717.
(9) Kinami, M.; Crenshaw, B. R.; Weder, C. *Chem. Mater.* **2006**, *18*, 946.
(10) Kunzelman, J.; Kinami, M.; Crenshaw, B. R.; Protasiewicz, J. D.; Weder, C. *Adv. Mater.* **2008**, *20*, 119.
(11) Davis, D. A.; Hamilton, A.; Yang, J.; Cremar, L. D.; Gough, D. V.; Potisek, S. L.; Ong, M. T.; Braun, P. V.; Martínez, T. J.; White, S. R.; Moore, J. S.; Sottos, N. R. *Nature* **2009**, *459*, 68.
(12) Weder, C. *Nature* **2009**, *459*, 45.
(13) Zhang, G.; Lu, J.; Sabat, M.; Fraser, C. L. *J. Am. Chem. Soc.* **2010**, *132*, 2160.
(14) Tsukuda, T.; Kawase, M.; Dairiki, A.; Matsumoto, K.; Tsubomura, T. *Chem. Commun.* **2010**, *46*, 1905.
(15) Schneider, J.; Lee, Y.-A.; Perez, J.; Brennessel, W. W.; Flaschenriem, C.; Eisenberg, R. *Inorg. Chem.* **2008**, *47*, 957.
(16) Lee, Y.; Eisenberg, R. *J. Am. Chem. Soc.* **2003**, *125* (26), 7778.
(17) Ito, H.; Saito, T.; Oshima, N.; Kitamura, N.; Ishizaka, S.; Hinatsu, Y.; Wakeshima, M.; Kato, M.; Tsuge, K.; Sawamura, M. *J. Am. Chem. Soc.* **2008**, *130*, 10044.
(18) Osawa, M.; Kawata, I.; Igawa, S.; Hoshino, M.; Fukunaga, T.; Hashizume, D. *Chem.—Eur. J.* **2010**, *16*, 12114.
(19) Perruchas, S.; Le Goff, X. F.; Maron, S. B.; Maurin, I.; Guillen, F. O.; Garcia, A.; Gacoin, T.; Boilot, J.-P. *J. Am. Chem. Soc.* **2010**, *132*, 10967.
(20) Du, P.; Knowles, K.; Eisenberg, R. *J. Am. Chem. Soc.* **2008**, *130*, 12576.
(21) Zhang, J.; Du, P.; Schneider, J.; Jarosz, P.; Eisenberg, R. *J. Am. Chem. Soc.* **2007**, *129*, 7726.
(22) Du, P.; Schneider, J.; Jarosz, P.; Zhang, J.; Brennessel, W. W.; Eisenberg, R. *J. Phys. Chem. B* **2007**, *111*, 6887.
(23) Du, P.; Schneider, J.; Jarosz, P.; Eisenberg, R. *J. Am. Chem. Soc.* **2006**, *128*, 7726.
(24) Furuta, P. T.; Deng, L.; Garon, S.; Thompson, M. E.; Fréchet, J. M. J. *J. Am. Chem. Soc.* **2004**, *126*, 15388.
(25) Chen, Z.; Wong, K. M.-C.; Kwok, E. C.-H.; Zhu, N.; Zu, Y.; Yam, V. W.-W. *Inorg. Chem.* **2011**, *50*, 2125.
(26) Yam, V. W.-W.; Tang, R. P.-L.; Wong, K. M.-C.; Ko, C.-C.; Cheung, K.-K. *Inorg. Chem.* **2001**, *40*, 571.
(27) Yam, V. W. W.; Tang, R. P. L.; Wong, K. M. C.; Cheung, K. K. *Organometallics* **2001**, *20*, 4476.
(28) Wong, K. M.-C.; Tang, W. S.; Lu, X.-X.; Yam, V. W.-W. *Inorg. Chem.* **2005**, *44*, 1492.
(29) Yang, Q.-Z.; Tong, Q.-X.; Wu, L.-Z.; Wu, Z.-X.; Zhang, L.-P.; Tung, C.-H. *Eur. J. Inorg. Chem.* **2004**, 1948.
(30) Lo, H.-S.; Yip, S.-K.; Wong, K. M.-C.; Zhu, N.; Yam, V. W.-W. *Organometallics* **2006**, *25*, 3537.
(31) Sun, R. W. Y.; Chow, A. L. F.; Li, X. H.; Yan, J. J.; Chui, S. S. Y.; Che, C. M. *Chem. Sci.* **2011**, *2*, 728.
(32) Wang, P.; Leung, C. H.; Ma, D. L.; Sun, R. W. Y.; Yan, S. C.; Chen, Q. S.; Che, C. M. *Angew. Chem., Int. Ed.* **2011**, *50*, 2554.
(33) Islam, A.; Sugihara, H.; Hara, K.; Singh, L. P.; Katoh, R.; Yanagida, M.; Takahashi, Y.; Murata, S.; Arakawa, H. *Inorg. Chem.* **2001**, *40*, 5371.
(34) Kwok, E. C.-H.; Chan, M.-Y.; Wong, K. M.-C.; Lam, W. H.; Yam, V. W.-W. *Chem.—Eur. J.* **2010**, *16*, 12244.
(35) Geary, E. A. M.; Yellowlees, L. J.; Jack, L. A.; Oswald, I. D. H.; Parsons, S.; Hirata, N.; Durrant, J. R.; Robertson, N. *Inorg. Chem.* **2005**, *44*, 242.
(36) Wong, K. M.-C.; Yam, V. W.-W. *Acc. Chem. Res.* **2011**, *44*, 424.
(37) Lu, W.; Chan, M. C. W.; Zhu, N. Y.; Che, C. M.; He, Z.; Wong, K. Y. *Chem.—Eur. J.* **2003**, *9*, 6155.
(38) Lu, W.; Chan, M. C. W.; Cheung, K. K.; Che, C. M. *Organometallics* **2001**, *20*, 2477.
(39) Connick, W. B.; Henling, L. M.; Marsh, R. E.; Gray, H. B. *Inorg. Chem.* **1996**, *35*, 6261.
(40) Grove, L. J.; Oliver, A. G.; Krause, J. A.; Connick, W. B. *Inorg. Chem.* **2008**, *47*, 1408.
(41) Grove, L. J.; Rennekamp, J. M.; Jude, H.; Connick, W. B. *J, Am. Chem. Soc.* **2004**, *126*, 1594.
(42) Yam, V. W.-W.; Chan, K.-Y.; Wong, K.-C.; Zhu, N. *Chem.—Eur. J.* **2005**, *11*, 4535.
(43) Muro, M. L.; Daws, C. A.; Castellano, F. N. *Chem. Commun.* **2008**, 6134.
(44) Du, P.; Schneider, J.; Brennessel, W. W.; Eisenberg, R. *Inorg. Chem.* **2008**, *47*, 69.
(45) Zhang, X.; Li, B.; Chen, Z.-H.; Chen, Z.-N. *J. Mater. Chem.* **2012**, *22*, 11427.
(46) Mathew, I.; Li, Y.; Li, Z.; Sun, W. *Dalton Trans.* **2010**, *39*, 11201.
(47) Field, J. S.; Grimmer, C. D.; Munro, O. Q.; Waldron, B. P. *Dalton Trans.* **2010**, *39*, 1558.
(48) Wadas, T. J.; Wang, Q.-M.; Kim, Y.-j.; Flaschenreim, C.; Blanton, T. N.; Eisenberg, R. *J. Am. Chem. Soc.* **2004**, *126*, 16841.
(49) Kobayashi, A.; Fukuzawa, Y.; Noro, S.-I.; Nakamura, T.; Kato, M. *Chem. Lett.* **2009**, 998.
(50) Rivera, E. J.; Barbosa, C.; Torres, R.; Grove, L.; Taylor, S.; Connick, W. B.; Clearfield, A.; Colón, J. L. *J. Mater. Chem.* **2011**, *21*, 15899.
(51) Ni, J.; Zhang, X.; Qiu, N.; Wu, Y.-H.; Zhang, L.-Y.; Zhang, J.; Chen, Z.-N. *Inorg. Chem.* **2011**, *50*, 9090.
(52) Ni, J.; Zhang, X.; Wu, Y.-H.; Zhang, L.-Y.; Chen, Z.-N. *Chem.—Eur. J.* **2011**, *17*, 1171.
(53) Abe, T.; Itakura, T.; Ikeda, N.; Shinozaki, K. *Dalton Trans.* **2009**, 711.
(54) *APEX2 v2009*; Bruker AXS: Madison, WI, 2009.
(55) Sheldrick, G. M. *Acta Crystallogr.* **2008**, *A64*, 112.
(56) Yam, V. W.-W.; Wong, K. M.-C.; Zhu, N. *J. Am. Chem. Soc.* **2002**, *124*, 6506.
(57) Yang, Q.-Z.; Wu, L.-Z.; Wu, Z.-X.; Zhang, L.-P.; Tung, C.-H. *Inorg. Chem.* **2002**, *41*, 5653.
(58) Lai, S.-W.; Lam, H.-W.; Lu, W.; Cheung, K.-K.; Che, C. M. *Organometallics* **2002**, *21*, 226.
(59) Yam, V. W.-W.; Hui, C.-K.; Wong, K. M.-C.; Zhu, N.; Cheung, K.-K. *Organometallics* **2002**, *21*, 4326.
(60) Yam, V. W.-W.; Wong, K. M.-C.; Zhu, N. *Angew. Chem., Int. Ed.* **2003**, *42*, 1400.
(61) Lu, W.; Chan, M. C. W.; Zhu, N.; Che, C.-M.; Li, C.; Hui, Z. *J. Am. Chem. Soc.* **2004**, *126*, 7639.
(62) Lai, S.-W.; Chan, M. C. W.; Cheung, K.-K.; Che, C.-M. *Inorg. Chem.* **1999**, *38*, 4262.

(63) Roundhill, D. M.; Gray, H. B.; Che, C. M. *Acc. Chem. Res.* **1989**, *22*, 55.